Totarol Inhibits Bacterial Cytokinesis by Perturbing the Assembly Dynamics of FtsZ †

ARTICLE *in* BIOCHEMISTRY · MAY 2007

Impact Factor: 3.02 · DOI: 10.1021/bi602573e · Source: PubMed

5 AUTHORS, INCLUDING:

Richa Jaiswal
Brandeis University
20 PUBLICATIONS **182** CITATIONS
SEE PROFILE

Renu Mohan
Sree Chitra Tirunal Institute for Medical Scie…
17 PUBLICATIONS **725** CITATIONS
SEE PROFILE

BIOCHEMISTRY

 Volume 46, Number 14 April 10, 2007

Articles

Totarol Inhibits Bacterial Cytokinesis by Perturbing the Assembly Dynamics of FtsZ†

Richa Jaiswal,‡ Tushar K. Beuria,‡ Renu Mohan,‡ Suresh K. Mahajan,§ and Dulal Panda*,‡

School of Biosciences and Bioengineering, Indian Institute of Technology, Bombay, Powai, Mumbai 400076, India, and Institute of Science, 15, Madam Cama Road, Mumbai 400032, India

Received December 15, 2006; Revised Manuscript Received February 6, 2007

ABSTRACT: Totarol, a diterpenoid phenol, has been shown to inhibit the proliferation of several pathogenic Gram-positive bacteria including *Mycobacterium tuberculosis*. In this study, totarol was found to inhibit the proliferation of *Bacillus subtilis* cells with a minimum inhibitory concentration of 2 μM. It did not detectably perturb the membrane structure of *B. subtilis*; it strongly induced the filamentation in *B. subtilis* cells, suggesting that it inhibits bacterial cytokinesis. Totarol (1.5 μM) reduced the frequency of the Z-ring occurrence per micrometer of the bacterial cell length but did not affect the nucleoid frequency, suggesting that it blocks cytokinesis by inhibiting the formation of the Z-ring. The assembly dynamics of FtsZ is thought to play an important role in the formation and functioning of the Z-ring, a machine that engineers cytokinesis in bacteria. Since totarol was shown to inhibit the proliferation of *M. tuberculosis*, we examined the effects of totarol on the assembly dynamics of *M. tuberculosis* FtsZ (*Mtb*FtsZ) in vitro. Totarol decreased the assembly of *Mtb*FtsZ protofilaments and potently suppressed the GTPase activity of *Mtb*FtsZ. It bound to *Mtb*FtsZ with a dissociation constant of 11 ± 2.3 μM. It increased the fluorescence intensity of the *Mtb*FtsZ−1-anilinonaphthalene-8-sulfonic acid complex and inhibited the fluorescence intensity of *N*-(1-pyrene)maleimide-labeled *Mtb*FtsZ, suggesting that totarol induces conformational changes in *Mtb*FtsZ. The results indicated that totarol can perturb the assembly dynamics of FtsZ protofilaments in the Z-ring. Totarol exhibited extremely weak inhibitory effects on HeLa cell proliferation. It did not affect microtubule organization in HeLa cells. The results suggest that totarol inhibits bacterial proliferation by targeting FtsZ and it may be useful as a lead compound to develop an effective antitubercular drug.

Cell division has always been an attraction for the drug development programs. One of the major targets of these drugs in higher eukaryotes has been the cytoskeletal protein tubulin (*1*−*2*). Tubulin plays a major role during eukaryotic cell division. Its prokaryotic homologue, FtsZ, is also shown to play a critical role in bacterial cell division (reviewed in refs *5*−*8*). FtsZ is known to be the first protein that reaches to the division site and polymerizes to form a cytokinetic ring, known as the "Z-ring" at the site of septum formation. The Z-ring is highly dynamic in nature (*9*). It helps in the recruitment of other accessory cell division proteins (*10*).

FtsZ is a highly conserved protein in the bacterial kingdom (*11*). Its conserved properties and similarities to tubulin implicate that FtsZ may be considered as a novel target for

†This work is supported by a Swarnajayanti fellowship, Department of Science and Technology, Government of India, to D.P. and a CSIR doctoral fellowship to R.J.

* Corresponding author. Tel: +91-22-2576-7838. Fax: +91-22-2572-3480. E-mail: panda@iitb.ac.in.

‡Indian Institute of Technology.

§ Institute of Science.

10.1021/bi602573e CCC: $37.00
Published on Web 03/10/2007

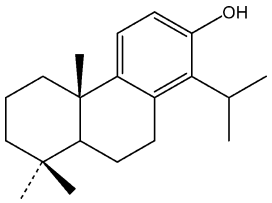

FIGURE 1: Structure of totarol (14-isopropyl-8,11,13-podocarpatrien-13-ol).

the antibacterial agents (*12*, *13*). Interestingly, most of the tubulin/microtubule targeting agents including paclitaxel, vinblastine, and colchicine do not affect FtsZ assembly dynamics, indicating that FtsZ can be a selective antibacterial target. Recently, a few attempts have been made to explore the utility of FtsZ as a target for antibacterial agents (*14*−*17*). Small molecule inhibitors that perturbed the functional properties of FtsZ from *Escherichia coli* (*14*, *16*) and *Mycobacterium tuberculosis* (*15*, *17*) were found to inhibit bacterial proliferation.

Totarol is a naturally occurring diterpenoid phenol extracted from *Podocarpus totara* (Figure 1). The timber of *P. totara* is known for its resilience against rotting, which is most likely derived from the antibacterial activity of totarol (*18*). Totarol has been found to exhibit a potent antibacterial activity against a number of Gram-positive bacteria, including *Staphylococcus aureus*, both the penicillin-susceptible and penicillin-resistant strains (*19*), and *M. tuberculosis* where it inhibited cell proliferation with a MIC of 16 μg/mL (*20*). Totarol was also found to potently inhibit the proliferation of *Propionibacterium acnes*, which causes skin diseases (*21*). Although totarol showed a potent antibacterial activity against a wide range of Gram-positive bacteria, it did not show any activity against Gram-negative bacteria. Totarol also has no activity against fungi. Totarol was shown to have a mild antitumor activity against the 9KB cell system, but the activity was too low to be of therapeutic value (*18*). Haraguchi et al. (*22*) proposed that totarol functions at the level of energy-coupled bacterial respiration, but later it was shown to inhibit the growth of facultative as well as obligate anaerobic bacteria under anaerobic conditions (*23*). Some studies on the mechanism of antibacterial activity of totarol claimed cell wall biosynthesis as a possible target. It has also been indicated that totarol may act by disrupting the phospholipid membrane of bacteria (*24*). Although different mechanisms for the antibacterial action of totarol have been proposed by several investigators (*22*, *24*, *25*), its antibacterial mechanism of action is far from clear.

Interestingly, we found that totarol increased the length of *Bacillus subtilis* cells by several fold, showing that it inhibits cell division in *B. subtilis*. At its effective inhibitory concentration range, totarol neither disrupted the membrane structure of *B. subtilis* cells nor detectably affected the nucleoid segregation. However, it perturbed the formation of the cytokinetic Z-ring, suggesting that the drug inhibits bacterial cytokinesis by perturbing the formation and functioning of the Z-ring. Totarol was found to bind to purified recombinant *M. tuberculosis* FtsZ (*Mtb*FtsZ).[1] It inhibited the assembly and GTPase activity of *Mtb*FtsZ in vitro. The data together indicated that totarol inhibits the proliferation of Gram-positive bacteria by targeting FtsZ.

MATERIALS AND METHODS

Materials. Totarol was purchased from Industrial Research Limited (New Zealand). HEPES [*N*-(2-hydroxyethyl)piperazine-*N*′-2-ethanesulfonic acid], monosodium glutamate, isopropyl β-D-thiogalactopyranoside (IPTG), bovine serum albumin (BSA), guanosine 5′-triphosphate (GTP), 4′,6-diamidino-2-phenylindole (DAPI), Cy3-conjugated goat anti-rabbit secondary antibody, and mouse monoclonal anti-α-tubulin antibody were obtained from Sigma (St. Louis, MO). 1-Anilinonaphthalene-8-sulfonic acid (ANS), *N*-(3-triethylammoniumpropyl)-4-[6-[4-(diethylamino)phenyl]hexatrienyl]-pyridinium dibromide (FM 4-64), 2′- (or 3′-) *O*-(trinitrophenyl)guanosine 5′-triphosphate (TNPGTP), *N*-(1-pyrene)maliemide (PM), and goat anti-mouse IgG−Alexa 568 were purchased from Molecular Probes (Eugene, OR). Primary polyclonal anti-FtsZ rabbit antibody was developed in rabbit against *E. coli* FtsZ by Bangalore Genie (India). All other chemicals used were of analytical grade.

*Expression and Purification of MtbFtsZ. Mtb*FtsZ was overexpressed and purified from the recombinant *E. coli* BL21 strain cloned in pET15b (kindly provided by Dr. P. Tonge and Dr. P. Nair) as described previously (*26*) with some modifications in the procedures. Briefly, the clear cell lysate was subjected to 33% ammonium sulfate precipitation. The pellet was dissolved in 25 mM HEPES−KOH buffer (pH 6.5) containing 2 mM $MgCl_2$, and the protein solution was desalted by passing through a preequilibrated gel filtration column (Bio-Gel P-6 column). *Mtb*FtsZ was purified using a Co^{2+} agarose column (BD biosciences) equilibrated with buffer A (50 mM HEPES−KOH, pH 7, plus 300 mM NaCl). The column was washed with 10−15 mL of buffer A. Recombinant *Mtb*FtsZ was eluted with 1 × elution buffer containing 150 mM imidazole, 50 mM HEPES−KOH (pH 7.0), and 300 mM NaCl. The protein solution was desalted using a preequilibrated Bio-Gel P-6 column. The N-terminal six-His tag was removed by digestion at 37 °C with 2 units of thrombin (Sigma)/mL of FtsZ (*26*). Thrombin was removed by passing the digested protein mixture over a benzamidine agarose column (Sigma; flow rate, 1 mL/min) equilibrated with desalting buffer containing 25 mM HEPES−KOH (pH 7.2), 100 mM KCl, 0.1 mM EDTA, 1 mM DTT, and 10% glycerol (*26*). *Mtb*FtsZ was further purified using one cycle of temperature-dependent glutamate-induced polymerization (*27*, *28*). The pellet was dissolved using ice-cold 25 mM HEPES buffer (pH 6.5) on ice. FtsZ concentration was measured by the Bradford method using BSA as a standard (*29*) and stored at −80 °C. The purity of FtsZ was estimated to be ∼98% from a Coomassie-stained SDS−PAGE.

Sedimentation Assay. Totarol was dissolved in 100% DMSO. *Mtb*FtsZ (6 μM) in 25 mM HEPES buffer, pH 6.5,

[1] Abbreviations: *Mtb*FtsZ, *Mycobacterium tuberculosis* FtsZ; HEPES, *N*-(2-hydroxyethyl)piperazine-*N*′-2-ethanesulfonic acid; IPTG, isopropyl β-D-thiogalactopyranoside; BSA, bovine serum albumin; GTP, guanosine 5′-triphosphate; DAPI, 4′,6-diamidino-2-phenylindole; ANS, 1-anilinonaphthalene-8-sulfonic acid; TNPGTP, 2′- (or 3′-) *O*-(trinitrophenyl)guanosine 5′-triphosphate; PM, *N*-(1-pyrene)maleimide.

was incubated in the absence and presence of different concentrations (10, 25, 50, and 75 μM) of totarol on ice for 30 min. Then, 100 mM KCl, 5 mM $MgCl_2$, and 1 mM GTP were added to the reaction mixtures and then polymerized at 37 °C for 30 min. The polymers were sedimented at 227000*g* for 30 min at 30 °C. The supernatant was collected without disturbing the pellet. The protein concentration in the supernatant was measured by Bradford's method (*29*) using BSA as a standard. The amount of polymer formed was calculated by subtracting the concentration of FtsZ in the supernatant from the total protein concentration (*27*).

Totarol-Induced Aggregation of MtbFtsZ. The preformed *Mtb*FtsZ aggregates were removed by centrifugation at 227000*g* for 30 min. *Mtb*FtsZ (6 μM) in 5 mM $MgCl_2$ and 25 mM HEPES buffer, pH 6.5, was incubated in the absence and presence of different concentrations of totarol on ice for 30 min. The reaction mixtures were then incubated at 37 °C for an additional 30 min and subsequently centrifuged at 227000*g* for 30 min at 30 °C. The supernatant was collected without disturbing the pellet. The protein concentration in the supernatant was measured. The amount of polymer formed was calculated by subtracting the concentration of FtsZ in the supernatant from the total protein concentration.

*Electron Microscopic Analysis. Mtb*FtsZ (6 μM) was incubated in the absence and presence of different concentrations (25 and 50 μM) of totarol in 25 mM HEPES, pH 6.5, buffer for 30 min on ice. After adding, 100 mM KCl, 5 mM $MgCl_2$, and 1 mM GTP were added to the reaction mixtures and were kept for polymerization at 37 °C for 30 min. After 30 min of assembly, FtsZ polymers in the samples were fixed with 0.5% glutaraldehyde, and 50 μL of the polymeric suspension was placed on the carbon-coated copper grids (300 mesh) and blotted dry. The grids were subsequently subjected to negative staining by 1% uranyl acetate solution and air-dried (*28*). The samples were examined using the FEI-Tecnai-G^2 12 electron microscope.

Measurement of the GTPase Activity. A malachite green ammonium molybdate assay was used to measure the production of inorganic phosphate during the GTP hydrolysis (*28*, *30*). *Mtb*FtsZ (6 μM) in 25 mM HEPES buffer (pH 6.5) was incubated in the absence and presence of different concentrations (5, 10, 25, 50, and 75 μM) of totarol on ice for 30 min. Subsequently, 100 mM KCl, 1 mM $MgCl_2$, and 1 mM GTP were added to the reaction mixtures, and the mixtures were immediately transferred to 37 °C. The GTP hydrolysis reaction was quenched after 30 min of incubation by adding 10% (v/v) of 7 M perchloric acid, and the quenched reaction solutions were kept on ice. The reaction mixtures were then kept at 25 °C for 10 min and incubated with malachite green ammonium molybdate solution at room temperature for 30 min. The production of phosphate ions was determined by measuring the absorbance at 650 nm. A phosphate standard curve was prepared using sodium phosphate.

Effect of TNPGTP on MtbFtsZ Assembly. Glutamate is known to induce the assembly and bundling of FtsZ polymers (*28*). *Mtb*FtsZ (9 μM) was polymerized in 1 M monosodium glutamate buffer, pH 6.8, containing 5 mM $MgCl_2$ and 100 mM KCl in the absence and presence of 150 μM TNPGTP for 30 min at 37 °C. Polymers were centrifuged at 227000*g* for 30 min at 30 °C. The protein concentration in the pellet was determined as described previously.

In addition, FtsZ (9 μM) was polymerized in 25 mM HEPES buffer, pH 6.5, containing 5 mM $MgCl_2$ and 100 mM KCl in the absence of glutamate without or with 150 μM TNPGTP. The polymers were collected by centrifugation, and the protein concentration in the pellet was determined as described previously.

Effect of Totarol on the Binding of TNPGTP to MtbFtsZ. TNPGTP, a fluorescent analogue of GTP, has been found to bind to FtsZ with a stoichiometry of ~0.84 TNPGTP per FtsZ monomer (*31*). Therefore, TNPGTP was used to determine the effect of totarol on the binding of GTP with *Mtb*FtsZ. *Mtb*FtsZ (5 μM) was incubated without or with different concentrations (10, 25, and 50 μM) of totarol in 25 mM HEPES buffer, pH 6.5, containing 5 mM $MgCl_2$ for 30 min on ice. TNPGTP (50 μM) was added to each of the reaction mixtures and incubated for an additional 4 h on ice. The fluorescence measurements were taken using 410 nm as the excitation wavelength. A cell of 0.3 cm path length was used to determine the fluorescence intensity changes.

*Determination of the Dissociation Constant of the Interaction between MtbFtsZ and Totarol. Mtb*FtsZ (1 μM) was incubated with different concentrations of totarol in 25 mM HEPES buffer, pH 6.5, at 25 °C for 30 min. Then, 50 μM ANS was added to each reaction mixture and incubated for an additional 30 min. The fluorescence intensity at 475 nm was measured using 360 nm as the excitation wavelength. A cell of 0.3 cm path length was used to determine the fluorescent intensity changes. Totarol increased the *Mtb*FtsZ−ANS complex fluorescence in a concentration-dependent manner. Totarol had no effect on the fluorescence intensity of free ANS in the absence of FtsZ. The increased fluorescence intensity of the *Mtb*FtsZ−ANS complex at 475 nm in the presence of totarol was used to determine the dissociation constant of the interaction between totarol and FtsZ (*32*, *34*). The fraction of binding sites (α) occupied by ANS was calculated using the equation:

$$\alpha = (F - F_0)/\Delta F_{max}$$

where F_0 is the fluorescence intensity of the *Mtb*FtsZ−ANS complex in the absence of totarol, F is the fluorescence intensity of the *Mtb*FtsZ−ANS complex in the presence of totarol, and ΔF_{max} is the maximum change in the fluorescence intensity when FtsZ is fully occupied with totarol. ΔF_{max} was determined by plotting $1/(F - F_0)$ versus 1/[totarol] and extrapolating 1/[totarol] to zero. The dissociation constant (K_d) was calculated using the equation:

$$1/\alpha = 1 + K_d/L_f$$

where L_f is the free totarol concentration and $L_f = L - \alpha$-[C], where L is the total concentration of totarol and [C] is the molar concentration of totarol-binding sites assuming a single binding site of totarol per FtsZ monomer.

Effect of Totarol on the Conformation of N-(1-Pyrene)-maleimide-Labeled MtbFtsZ. MtbFtsZ (6 μM) was incubated with 6 μM *N*-(1-pyrene)maleimide (PM) in 25 mM HEPES buffer, pH 6.5, for 2 h on ice. The reaction mixture was then passed through a gel filtration column (Bio-Gel P-6) to remove the free PM. The concentration of *Mtb*FtsZ-bound PM was estimated from the absorbance at 337 nm using a molar extinction coefficient of 37000 M^{-1} cm^{-1} at 337 nm.

The protein concentration was measured by Bradford's method (*28*). The incorporation ratio of PM per mole of *Mtb*FtsZ was determined by dividing the bound PM concentration by the *Mtb*FtsZ concentration. The incorporation ratio (PM/FtsZ) was found to be 0.5 ± 0.2. PM−*Mtb*FtsZ (1 μM) was incubated in the absence and presence of different concentrations (5, 10, 25, and 50 μM) of totarol at 25 °C for 30 min. Fluorescence spectra were taken using 337 nm as the excitation wavelength. Totarol had no effect on the fluorescence intensity of 2-mercaptoethanol-conjugated PM.

Antibacterial Assay. The overnight grown culture was used to inoculate 10 mL of LB medium in a way that the final OD_{600} of the media reached ~0.1. Totarol was dissolved in 100% DMSO and sterilized by passing through a 0.2 μm syringe filter (Nalgene); the final concentration of DMSO in all experiments was 0.1%. Different concentrations (0.5, 1.0, 1.5, 2, and 3 μM) of totarol were added to culture, and the cell proliferation was observed at different time intervals by measuring the OD_{600}. OD_{600} values were used to calculate the percentage inhibition in the cell growth with respect to control. To determine the MIC (minimum inhibitory concentration) of totarol, *B. subtilis* 168 cells were grown for 2 h in the absence and presence of different concentrations of totarol (0.5, 1.0, 1.5, 2, and 3 μM). Then appropriate dilutions were spread on the LB agar plates. The plates were incubated for 12 h at 37 °C. The number of colonies growing on each plate was determined using a bacteriological colony counter (Medica Instrument Co., India).

Visualization of Bacterial Morphology. An overnight culture was used to inoculate tubes containing 10 mL of LB medium and different concentrations (0.5, 1.0, and 1.5 μM) of totarol. Cells were grown for 2 h and fixed as described (*14*). The cells were examined using differential interference contrast microscopy.

Membrane Staining. FM4-64, a fluorescent dye, was used to stain the membranes (*14*). Briefly, *B. subtilis* 168 cells were grown in the absence and presence of different concentrations of totarol for 2 h. FM4-64 was added to the growing cultures. The cells were grown for an additional 15 min and observed under an Eclipse TE-2000 U microscope (Nikon). The images were analyzed using Image Pro Plus software (Media Cybernetics, Silver Spring, MD).

Immunofluorescence Microscopy. The Z-ring and nucleoids of *B. subtilis* 168 cells were visualized in the absence and presence of totarol as described previously (*14*). Briefly, *B. subtilis* 168 cells were grown in LB media for overnight. The cells were diluted in LB media in the absence and presence of different concentrations (0.5, 1.0, and 1.5 μM) of totarol and further grown for 2 h. Cells were fixed using 2.5% formaldehyde and 0.04% glutaraldehyde. FtsZ was stained with polyclonal anti-FtsZ rabbit antibody followed by Cy3-conjugated goat anti-rabbit secondary antibody. Nucleoids were stained using 1 μg/mL DAPI and visualized under a fluorescence microscope (Eclipse TE-2000 U microscope; Nikon).

Binding of Totarol with Tubulin. The binding interaction of totarol with tubulin was examined by monitoring the effects of totarol on the intrinsic tryptophan fluorescence of tubulin (*3*, *34*). Goat brain tubulin (1 μM) was incubated without or with different concentrations of totarol in 25 mM PIPES, pH 6.5, for 30 min at 25 °C. The fluorescence intensity at 335 nm was measured using 295 nm as the excitation wavelength.

Mammalian Cell Proliferation Assay. HeLa cells were grown in minimal essential medium (Himedia) supplemented with 10% (v/v) fetal bovine serum, 1.5 g/L sodium bicarbonate, and 1% antibiotic antimycotic solution at 37 °C in a humidified atmosphere of 5% carbon dioxide (*35*). The inhibition of cell proliferation was determined using a standard sulforhodamine B assay as described previously (*35*, *36*). The cells were seeded at a density of 1×10^5 cells/mL and were grown in the absence and presence of different concentrations (1−50 μM) of totarol for 24 h. DMSO was used as a vehicle control. The cells were fixed with 10% trichloroacetic acid and stained with 0.4% sulforhodamine B, and the concentration of the protein-bound dye was determined by measuring the absorbance at 560 nm (*35*).

Immunofluorescence Microscopy of Mammalian Cells. Immunofluorescence microscopy was performed as described previously (*33*, *35*). Briefly, the cells were grown on coverslips and incubated with different concentrations of totarol for one cell cycle. The cells were then fixed and permeabilized as described previously (*33*). After nonspecific sites were blocked with 2% BSA/PBS, the cells were incubated with the mouse monoclonal anti-α-tubulin antibody for 2 h at 25 °C followed by the Alexa 568-conjugated anti-mouse IgG antibody for 1 h at 25 °C. To visualize nuclei, the cells were incubated with DAPI and examined with a Nikon Eclipse TE-2000 U fluorescence microscope. The images were analyzed by using Image Pro Plus software (Media Cybernetics, Silver Spring, MD).

RESULTS

Effects of Totarol on Polymerization of MtbFtsZ. The effect of totarol on the polymerization of *Mtb*FtsZ was analyzed by quantifying the polymerized mass of FtsZ in the absence and presence of different concentrations (10−75 μM) of totarol. Under the experimental conditions used, 75% of the total FtsZ was sedimented as polymers in the absence of totarol. Totarol decreased the amount of polymerized FtsZ (Figure 2). For example, 50 μM totarol inhibited the polymerized mass of FtsZ by 27% ($p < 0.001$).

The effect of totarol on the assembly of *Mtb*FtsZ protofilaments was also examined using a transmission electron microscope. The number of FtsZ polymers per field of view was found to be reduced significantly in the presence of totarol, suggesting that totarol reduced the assembly of FtsZ (Figure 3). The average width of *Mtb*FtsZ protofilaments was determined to be 20 ± 12 nm. Totarol had no significant effect on the width of the FtsZ protofilaments (data not shown).

Further, totarol was found to induce aggregation of *Mtb*FtsZ monomers under nonassembly conditions in the absence of GTP. For example, under the nonassembly conditions used, 8 ± 1%, 18 ± 6%, and 39 ± 2% of *Mtb*FtsZ were sedimented as polymers in the absence and presence of 50 and 100 μM totarol, respectively. In addition, the electron micrographs showed that high concentrations of totarol caused extensive aggregation of FtsZ monomers (Figure 3C). The findings together may explain the modest effect of totarol on the assembly of FtsZ in vitro as determined by the sedimentation analysis.

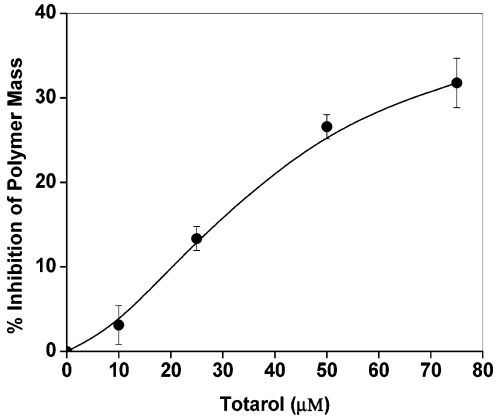

FIGURE 2: Effects of totarol on the assembly of *Mtb*FtsZ. *Mtb*FtsZ (6 μM) was polymerized in 25 mM HEPES buffer, pH 6.5, containing 100 mM KCl, 5 mM $MgCl_2$, and 1 mM GTP in the absence and presence of different concentrations of totarol for 30 min at 37 °C as described in Materials and Methods. The polymers were collected by centrifugation at 227000*g* for 30 min. The polymeric mass of *Mtb*FtsZ was determined by subtracting the supernatant protein concentration from the total protein concentration. The experiment was performed four times.

Totarol Suppressed the GTPase Activity of MtbFtsZ but Did Not Affect the Binding of GTP to MtbFtsZ. It is thought that the assembly dynamics of FtsZ is regulated by the GTP hydrolysis (*37*, *38*). Totarol was found to reduce the GTPase activity of *Mtb*FtsZ in a concentration-dependent manner (Figure 4). For example, 10 and 75 μM totarol reduced the GTPase activity of *Mtb*FtsZ by 24% and 67%, respectively, compared to the control ($p < 0.001$). The results suggested that totarol perturbs the assembly dynamics of FtsZ.

Totarol might inhibit the GTP hydrolysis rate of FtsZ assembly either by inhibiting the binding of GTP to FtsZ or by modulating assembly dynamics of FtsZ protofilaments. The effect of totarol on the GTP binding was determined by using TNPGTP, a fluorescent analogue of GTP. The fluorescence intensity of TNPGTP was found to increase by 70% upon binding to *Mtb*FtsZ. Preincubation of *Mtb*FtsZ with GTP strongly inhibited the development of TNPGTP fluorescence, suggesting that TNPGTP binds to *Mtb*FtsZ at the GTP site (Figure 5A).

Using two different assembly conditions, we examined whether TNPGTP could induce the assembly of *Mtb*FtsZ. In the first approach, *MtbFtsZ* was polymerized in 25 mM HEPES buffer containing 5 mM $MgCl_2$ and 100 mM KCl in the absence and presence of 150 μM TNPGTP. In the presence of TNPGTP, 15 $\pm$ 0.5% of the total FtsZ formed sedimentable polymers. However, only 3 $\pm$ 1.8% of the total FtsZ formed sedimentable polymers in the absence of TNPGTP, indicating that TNPGTP could promote the assembly of *Mtb*FtsZ. In the second approach, the effect of TNPGTP on the glutamate-induced assembly of *Mtb*FtsZ was analyzed. TNPGTP was found to promote the assembly of *Mtb*FtsZ strongly in the presence of monosodium glutamate. Under the conditions used, 9 $\pm$ 3% and 83 $\pm$ 2% of the total FtsZ were sedimented as polymers in the absence and presence of 150 μM TNPGTP, respectively. The results together suggested that TNPGTP can be used as a probe to monitor the GTP binding site on *Mtb*FtsZ. Totarol did not change the fluorescence intensity of FtsZ-bound TNPGTP significantly, suggesting that totarol does not affect the binding of GTP to FtsZ (Figure 5B).

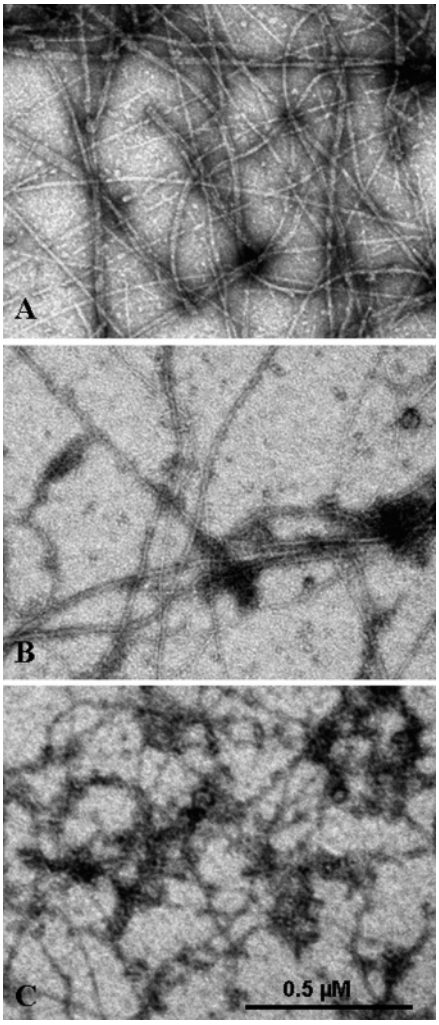

FIGURE 3: Electron micrographs of *Mtb*FtsZ polymers formed at different totarol concentrations. FtsZ (6 μM) was polymerized in 25 mM HEPES buffer, pH 6.5, containing 100 mM KCl, 5 mM $MgCl_2$, and 1 mM GTP at 37 °C in the absence and presence of totarol (25 and 50 μM) for 30 min. Shown are electron micrographs of FtsZ polymers formed in the absence (A) and presence of 25 μM (B) and 50 μM (C) totarol. The scale bar = 500 nm.

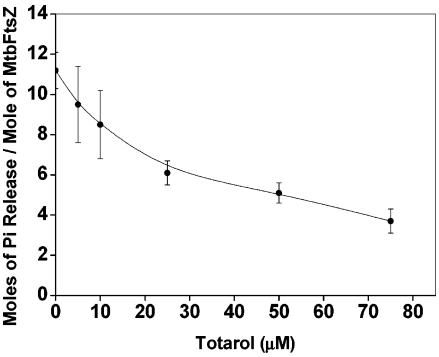

FIGURE 4: Effect of totarol on the GTPase activity of *Mtb*FtsZ. FtsZ (6 μM) was incubated in 25 mM HEPES buffer (pH 6.5) containing 100 mM KCl and 5 mM $MgCl_2$ in the absence and presence of totarol (5−75 μM) for 30 min on ice. Then, 1 mM GTP was added to the reaction mixtures and immediately transferred to 37 °C. Samples were taken out after 30 min, and the hydrolysis reaction was quenched by adding perchloric acid. The production of phosphate ions was determined by measuring the absorbance at 650 nm. The data are an average of four experiments.

*Interaction of Totarol with MtbFtsZ. Mtb*FtsZ does not have a tryptophan residue. ANS, a hydrophobic probe, is

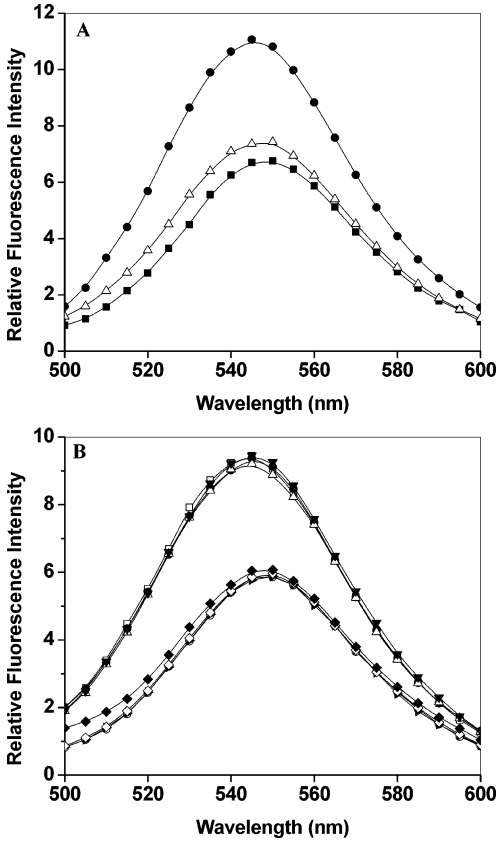

FIGURE 5: Effect of totarol on the binding of TNPGTP to *Mtb*FtsZ. *Mtb*FtsZ (7 μM) in 25 mM HEPES buffer containing 5 mM $MgCl_2$ was incubated without or with 2 mM GTP for 30 min on ice. Then, 40 μM TNPGTP was added to the reaction mixtures and incubated for an additional 2 h on ice. Fluorescence spectra of TNPGTP in the absence (■) and presence of *Mtb*FtsZ without (●) or with 2 mM GTP (Δ) are shown in panel A. Panel B represents the effect of totarol on the fluorescence intensity of TNPGTP. FtsZ (5 μM) was incubated in the absence and presence of different concentrations of totarol as described in Materials and Methods. Then, 50 μM TNPGTP was added to the reaction mixtures and incubated for an additional 4 h. Fluorescence spectra were taken using 410 nm as the excitation wavelength. The emission spectra of free TNPGTP in the absence (○) and presence of 10 μM (arrowhead), 25 μM (◇), and 50 μM (◆) totarol and the emission spectra of *Mtb*FtsZ-bound TNPGTP in the absence (□) and presence of 10 μM (●), 25 μM (Δ), and 50 μM (▼) totarol are shown in panel B. The experiment was performed four times.

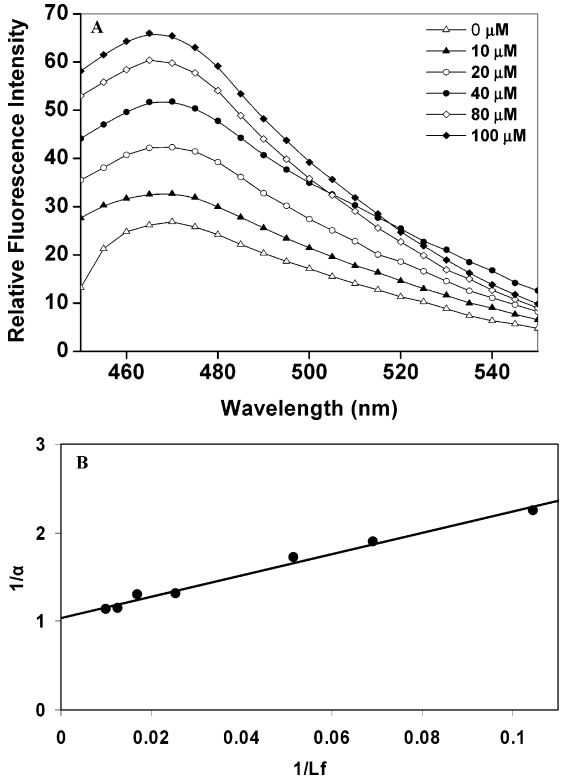

FIGURE 6: Binding of totarol to *Mtb*FtsZ. The emission spectra of the *Mtb*FtsZ−ANS complex in the absence (Δ) and presence of 10 μM (▲), 20 μM (○), 40 μM (●), 80 μM (◇), and 100 μM (◆) totarol are shown in panel A. The double reciprocal plot of the binding data is shown in panel B. The excitation and emission wavelengths were 360 and 475 nm, respectively. The experiment was performed nine times.

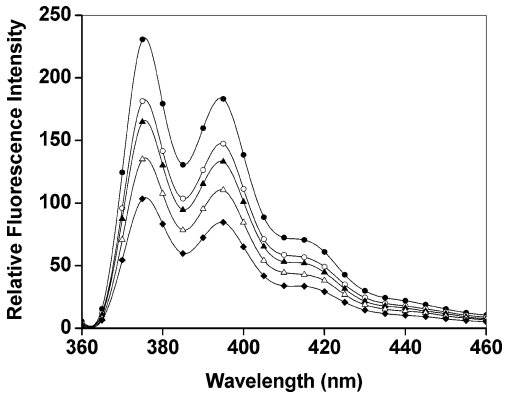

FIGURE 7: Effect of totarol on the fluorescence of PM−*Mtb*FtsZ. PM−*Mtb*FtsZ (1 μM) was incubated in the absence and presence of different concentrations of totarol. Fluorescence spectra were taken using 337 nm as the excitation wavelength. Shown are the fluorescence intensity of PM−*Mtb*FtsZ in the absence (●) and presence of 5 μM (○), 10 μM (▲), 25 μM (Δ), and 50 μM (◆) totarol. The experiment was repeated three times.

routinely used to determine the binding of a ligand to a protein (*32*, *33*). It has been shown that ANS had no effect on the polymerization properties of FtsZ (*39*). Therefore, ANS was used to determine the interaction between *Mtb*FtsZ and totarol. ANS was found to bind to *Mtb*FtsZ (Figure 6A). Totarol increased the fluorescence intensity of the *Mtb*FtsZ−ANS complex in a concentration-dependent manner, indicating that it induced conformational change in the protein (Figure 6A). Using a double reciprocal plot of the fluorescence data, the dissociation constant for the binding of totarol to *Mtb*FtsZ was calculated to be 11 ± 2.3 μM (Figure 6B).

*Mtb*FtsZ has a single cysteine residue at its 155th position. The single Cys155 residue of *Mtb*FtsZ was covalently modified using PM, a sulfhydryl-specific reagent. Totarol reduced the fluorescence intensity of the PM−*Mtb*FtsZ complex in a concentration-dependent manner, indicating that it induced conformational change in the protein (Figure 7).

Inhibition of Cell Proliferation of B. subtilis and Induction of Filamentation by Totarol. M. tuberculosis is a Gram-positive pathogenic bacterium. We used *B. subtilis* 168 cells as a nonpathogenic Gram-positive model to probe whether totarol can inhibit Z-ring formation in bacteria by inhibiting FtsZ assembly; moreover, *B. subtilis* FtsZ shares 58% amino acid identity with *Mtb*FtsZ. Totarol inhibited the cell proliferation of *B. subtilis* 168 and caused cell elongation. In liquid broth medium the growth was reduced by 17 ± 6%, 55 ± 5%, and nearly 100% in the presence of 1, 1.5, and 2 μM totarol, respectively. The MIC value of totarol for *B. subtilis* was found to be 2 μM calculated using the

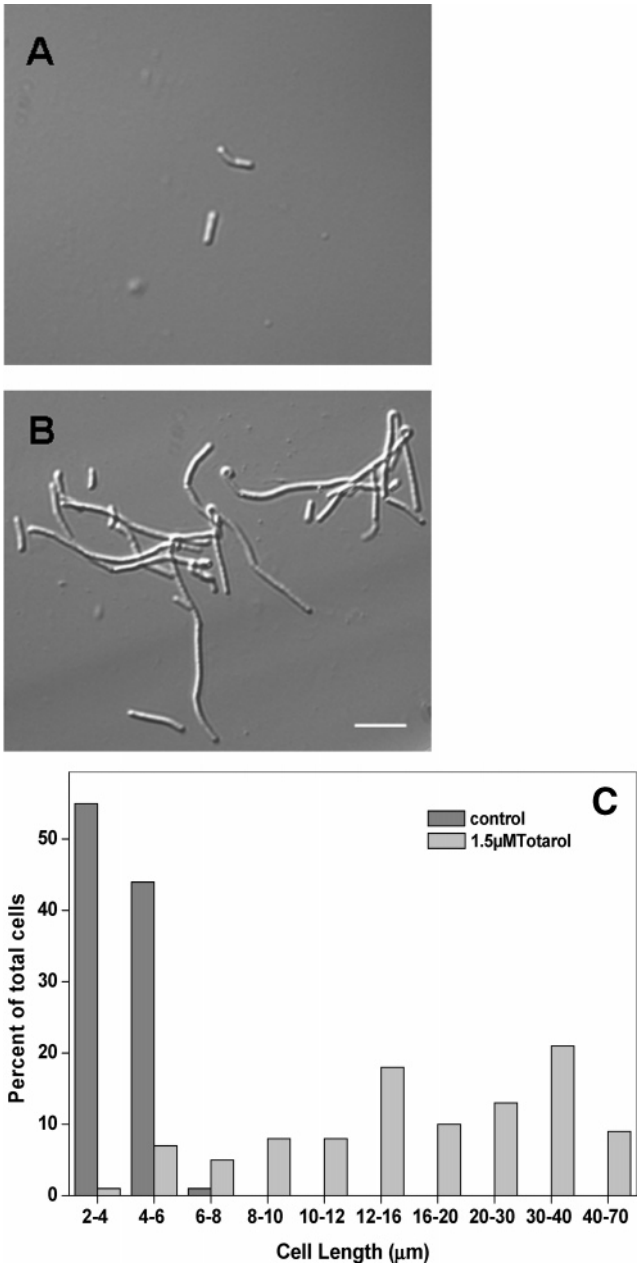

FIGURE 8: Totarol-induced filament formation in *B. subtilis* 168. *B. subtilis* 168 cells were grown for 2 h in the absence (A) and in the presence of 1.5 μM (B) totarol in LB media. The morphology of cells was observed under differential interference contrast microscopy. The scale bar is 10 μm. The effects of the totarol on the length of *B. subtilis* 168 cells are shown in panel C. The dark gray bar represents control cells, and the light gray bar represents cells treated with 1.5 μM totarol.

colony count method (*40*, *41*). MIC is calculated as the lowest concentration of totarol that gave no visible colonies when parallel control plates with no totarol gave 200 $\pm$ 20 colonies. Totarol also caused lengthening in cell size of *B. subtilis* (Figure 8A,B). The incubation of *B. subtilis* 168 cells with 1.5 μM totarol for 2 h increased the cell length by 5-fold from 3.9 $\pm$ 1.0 μm to 22.4 $\pm$ 1 4.8 μm, in the absence and presence of totarol, respectively (Figure 8C). In the absence of totarol, 55%, 44%, and 1% of the cells were found to be within 2$-$4, 4$-$6, and 6$-$8 μm length, respectively. In the presence of 1.5 μM totarol, 1% cells were found to be within 2$-$4 μm length, 12% and 16% cells were having cell length between 4$-$8 and 8$-$12 μm, respectively, while the length of 71% cells ranged from 12 to 70 μm. The results indicated that totarol inhibits bacterial proliferation by blocking cytokinesis.

The effect of totarol on the membrane of *B. subtilis* 168 cells was examined using a membrane-staining dye FM 4-64. The fluorescence intensity of the dye across the membrane of *B. subtilis* 168 was compared in the absence and in the presence of 0.5, 1, and 1.5 μM totarol. The fluorescence intensities across the membrane were found to be 1579 $\pm$ 283 (au), 1657 $\pm$ 421 (au), 1514 $\pm$ 464 (au), and 1487 $\pm$ 350 (au) in the absence and presence of 0.5, 1, and 1.5 μM totarol, respectively. The observation suggested that totarol did not affect the membrane integrity of *B. subtilis* 168 detectably.

Totarol Inhibited Z-Ring Formation but Did Not Perturb Nucleoid Segregation. Since totarol appeared to inhibit bacterial cytokinesis, the effects of totarol on the Z-ring assembly were analyzed along with its effects on the nucleoid segregation. *B. subtilis* 168 cells were grown in the absence and presence of 1.5 μM totarol for 2 h. Cells were immunostained with anti-FtsZ antibody, and nucleoids were stained with DAPI as described in Materials and Methods. Most of the control cells were found to contain two nucleoids. For example, 13%, 76%, and 11% of the control cells were found to have one, two, and four nucleoids, while in the presence of 1.5 μM totarol, cells with one nucleoid were not found and 38%, 32%, and 30% cells were found to contain two, four, and eight or more nucleoids, respectively. Thus, in contrast to the control cells, a significant population of the totarol-treated cells had four and eight or more nucleoids. Further, in control cells 13% of the cells were with one nucleoid with an average length of 2.7 $\pm$ 0.2 μm, which reflects the population of newborn cells. Whereas in the case of totarol-treated cells, no cell was found with one nucleoid, suggesting that totarol inhibited cell division. The frequency of nucleoid/μm of cell length was found to be 0.48 $\pm$ 0.01 and 0.45 $\pm$ 0.01 in the absence and presence of 1.5 μM totarol, indicating that totarol had no detectable effect on the nucleoid segregation of bacteria ((Figure 9 and Table 1).

A majority (85%) of the control cells with two nucleoids had a prominent Z-ring at the mid-cell. In the absence of totarol, 69% of the control cells had one Z-ring whereas in the presence of 1.5 μM totarol only 20% of the cells were found to contain a Z-ring (Figure 9). Further, the Z-rings were found to be perturbed in the presence of totarol. The frequencies of the Z-ring/μm of the bacterial cells in the absence and presence of totarol were determined to be 0.16 $\pm$ 0.009 and 0.03 $\pm$ 0.005, respectively (Table 1). Thus, totarol strongly decreased the frequency of the Z-ring occurrence/μm of the bacterial cell length and did not affect the frequency of nucleoid/μm of cell length, suggesting that it inhibits bacterial cytokinesis by perturbing the formation and functioning of the Z-ring.

Totarol Does Not Bind to Tubulin. In contrast to the effects of totarol on the intensity of the FtsZ$-$ANS complex (Figure 6A), totarol (10 and 25 μM) did not detectably influence the fluorescence intensity of the tubulin$-$ANS complex (data not shown). Tubulin contains eight tryptophan residues. Therefore, the intrinsic tryptophan fluorescence of tubulin was used to determine the binding of totarol to tubulin. Totarol had minimal effects on the intrinsic tryptophan

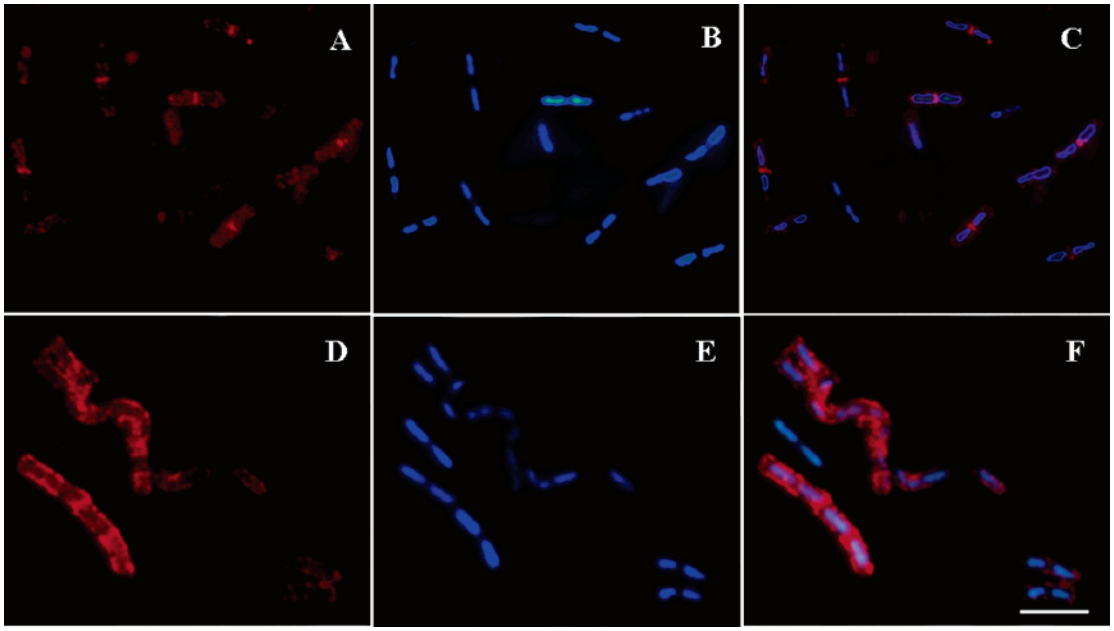

FIGURE 9: Effects of totarol on the Z-ring and nucleoid segregation. Cells were immunostained with polyclonal anti-FtsZ rabbit antibody followed by Cy3-conjugated goat anti-rabbit secondary antibody and visualized under a fluorescence microscope as described in Materials and Methods. Nucleoids were visualized by treating the cells with DAPI. The Z-rings are shown in red, and the DAPI-stained nucleoids are shown in blue. Shown are control cells (A and B) and overlay (C) and in the presence of 1.5 μM totarol (D and E) and overlay (F). The scale bar is 5 μm.

Table 1: Effects of Totarol on the Z-Ring and Nucleoids of *B. subtilis* 168[a]

description	control	totarol (1.5 μM)
% of cells with a Z-ring	69	20
frequency of Z-rings/μm of the cell length	0.16 ± 0.009	0.03 ± 0.005
frequency of nucleoids/μm of the cell length	0.48 ± 0.01	0.45 ± 0.01
% of cells containing two nucleoids	75.7	38
% of cells with two nucleoids having a Z-ring	85	21
frequency of Z-ring /μm of the cells containing two nucleoids	0.23 ± 0.005	0.05 ± 0.01

[a]A minimum of 150 cells were scored in the case of the control as well as in the presence of 1.5 μM totarol.

fluorescence of tubulin (data not shown). For example, 50 μM totarol decreased the intrinsic tryptophan fluorescence of tubulin by 9%, suggesting that totarol does not bind to tubulin effectively.

Effect of Totarol on Mammalian Cell Proliferation and Cell Division. Totarol inhibited HeLa cell proliferation very weakly. The half-maximal inhibition (IC_{50}) was calculated to be 18 ± 1 μM, which is 9 times higher than the MIC calculated for the *B. subtilis* 168 cell proliferation (2 μM). The effects of totarol on the microtubules and chromosomes of the HeLa cells were analyzed by immunofluorescence microscopy using anti-tubulin antibodies and DAPI staining of the chromosomes. Totarol (20 and 50 μM) did not produce any detectable effect on the microtubules and chromosomes of the HeLa cells. The organization of microtubules and chromosomes of the totarol-treated cells was found to be similar to that of the control cells (data not shown). These results show that totarol inhibited mammalian cell proliferation weakly and did not cause any change in the microtubules as well as the chromosome structure of the mammalian cells.

DISCUSSION

In this study, totarol was found to exert differential inhibitory effects on the proliferation of mammalian and bacterial cells. Totarol bound to purified *Mtb*FtsZ and inhibited the assembly and GTPase activity of *Mtb*FtsZ protofilaments in vitro, suggesting that it can perturb the assembly dynamics of FtsZ in bacteria. Further, totarol inhibited the proliferation of *B. subtilis* cells at cytokinesis and perturbed the formation and functioning of the Z-ring, indicating that it inhibits bacterial proliferation by inhibiting the assembly dynamics of FtsZ protofilaments in the Z-ring.

Recent studies indicated that several small organic molecules including viriditoxin, zantrins, SRI 3072, dichamanetin, and sanguinarine inhibit bacterial cell division by perturbing FtsZ assembly properties (*14*−*17*, *42*). For example, dichamanetin, SRI 3072, and taxane derivatives are found to inhibit proliferation of *B. subtilis* cells with MIC values of 1.7, ~0.28, and 2.5 μM, respectively (*17*, *42*, *43*). Totarol was found to inhibit *B. subtilis* proliferation with a MIC of 2 μM (present study), and it was shown to inhibit the proliferation of several pathogenic bacteria, such as *S. aureus*, *P. acnes*, and *Streptococcus mutans*, with MIC values of 5.4, 2.7, and 1.4 μM, respectively (*19*). Thus, the antibacterial activity of totarol is comparable to that of other known FtsZ inhibitors.

Totarol increased the fluorescence intensity of the FtsZ−ANS complex and decreased the fluorescence intensity of PM−FtsZ, indicating that the binding of totarol induced conformational changes in FtsZ. Although totarol was found to bind to *Mtb*FtsZ with a modest affinity (K_d = 11 ± 2.3 μM), high concentrations of totarol were required to inhibit the assembly of *Mtb*FtsZ in vitro. For example, 75 μM totarol inhibited the assembly of purified *Mtb*FtsZ by 32%. One can estimate that under these conditions ~80% of the soluble *Mtb*FtsZ should be complexed with totarol. Therefore, the binding of totarol to *Mtb*FtsZ does not

inactivate the protein by sequestering it. The *Mtb*FtsZ−totarol complex copolymerizes along with MtbFtsZ into the protofilaments, and the incorporation of a significant number of *Mtb*FtsZ−totarol complexes in the polymer inhibits the polymerization of *Mtb*FtsZ. The inhibition of the assembly of *Mtb*FtsZ protofilaments by totarol was likely to be due to the conformational changes that occurred in the protein upon ligand binding. Alternatively, the presence of totarol, a bulky molecule, on the surface of FtsZ may prevent further addition of FtsZ molecules by steric hindrance. It is also possible that the presence of totarol on the FtsZ surface prevents the binding of FtsZ to an accessory protein that regulates FtsZ assembly dynamics in bacteria.

The GTPase activity of purified *Mtb*FtsZ was inhibited by 50% in the presence of 40 μM totarol while it inhibited the growth of *B. subtilis* cells with a MIC of 2 μM. Thus, the concentration required to inhibit *B. subtilis* proliferation by totarol was found to be considerably lower than the concentration required to inhibit either GTPase activity of purified FtsZ or assembly of FtsZ in vitro. Similar differences in the concentrations required for inhibiting bacterial proliferation and the assembly and GTPase activity of FtsZ in vitro have been observed for several of the FtsZ-targeted antibacterial agents (*15*, *17*, *42*). For example, 100 μM SRI-3072 was required to inhibit the GTPase activity of FtsZ by 20% while the agent inhibited the proliferation of *M. tuberculosis* with a MIC of 0.28 μM (*17*). Dichamanetin (12.5 μM) decreased the GTPase activity of FtsZ by 50% while it inhibited the proliferation of *B. subtilis* cells with a MIC of 1.7 μM (*42*). Similarly, zantrins decreased the GTPase activity of *Mtb*FtsZ by 50% at 50 μM, whereas they possessed MIC of 2.5 μM against *B. subtilis* (*15*). One of the possible reasons for the stronger antibacterial activity of totarol compared to its effects on the assembly of purified FtsZ in vitro is that the intracellular concentration of totarol is likely to be much higher than the concentration of the agent in the media. Alternatively, totarol might bind to *B. subtilis* FtsZ with stronger affinity than to *Mtb*FtsZ. Another attractive possibility is that the binding of totarol with FtsZ perturbs the binding of FtsZ and its interacting partner(s), which inhibits the formation and functioning of the cytokinetic Z-ring in bacteria.

Totarol did not perturb the membrane staining of *B. subtilis* cells detectably, and it increased the average length of *B. subtilis* cells. The results together suggested that the antibacterial activity of totarol was not likely to be associated with a major perturbation in the membrane structure of the bacteria. At its effective concentration (1.5 μM), totarol did not alter the frequency of occurrence of nucleoids per micrometer of the cell length, suggesting that it did not detectably affect replication and segregation of nucleiods. The same concentration of totarol strongly inhibited the formation of the cytokinetic Z-ring, suggesting that totarol inhibited bacterial cytokinesis by perturbing the formation and functioning of the Z-ring.

Totarol exerted extremely weak inhibitory effects on mammalian cell proliferation. It did not bind to purified tubulin effectively, and high concentrations of totarol did not perturb microtubule and chromosome organization in the HeLa cells. The results together suggested that totarol exerted differential activity toward eukaryotic and prokaryotic cells; therefore, it may be considered as a lead compound for developing FtsZ-targeted antibacterial agents.

Tuberculosis is one of the most infectious deadly diseases across the world. Due to irregular or inadequate chemotherapy, drug-resistant strains of *M. tuberculosis* have emerged as an enormous danger for the survival of millions of affected people. There is an urgent need to discover new antitubercular drugs with a novel mechanism of action. Since FtsZ plays an essential role in bacterial cell division and it is a highly conserved protein, FtsZ-targeted drugs may overcome the drug resistance problems of the traditionally used antitubercular drugs (*11*). The evidence presented in this study suggested that totarol inhibits bacterial proliferation by inhibiting the formation and functioning of the cytokinetic Z-ring through its binding to FtsZ and that totarol can be used as a tool to elucidate the role of FtsZ assembly dynamics in bacterial cytokinesis.

ACKNOWLEDGMENT

We thank SAIF, IIT Bombay, for providing the electron microscopy facility.

REFERENCES

1. Bhalla, K. N. (2003) Microtubule-targeted anticancer agents and apoptosis, *Oncogene 22*, 9075−9086.
2. Nagle, A., Hur, W., and Gray, N. S. (2006) Antimitotic agents of natural origin, *Curr. Drug Targets 7*, 305−326.
3. Panda, D., Rathinasamy, K., Santra, M. K., and Wilson, L. (2005) Kinetic suppression of microtubule dynamic instability by griseofulvin: implications for its possible use in the treatment of cancer, *Proc. Natl. Acad. Sci. U.S.A. 102*, 9878−9883.
4. Wilson, L., and Jordan, M. A. (2004) New microtubule/tubulin-targeted anticancer drugs and novel chemotherapeutic strategies, *J. Chemother. 16*, 83−85.
5. Addinall, S. G., and Holland, B. (2002) The tubulin ancestor, FtsZ, draughtsman, designer and driving force for bacterial cytokinesis, *J. Mol. Biol. 318*, 219−236.
6. Lowe, J., van den Ent, F., and Amos, L. A. (2004) Molecules of the bacterial cytoskeleton, *Annu. Rev. Biophys. Biomol. Struct. 33*, 177−198.
7. Michie, K. A., and Lowe, J. (2006) Dynamic filaments of the bacterial cytoskeleton, *Annu. Rev. Biochem. 75*, 467−492.
8. Margolin, W. (2005) FtsZ and the division of prokaryotic cells and organelles, *Nat. Rev. Mol. Cell Biol. 6*, 862−871.
9. Stricker, J., Maddox, P., Salmon, E. D., and Erickson, H. P. (2002) Rapid assembly dynamics of the *Escherichia coli* FtsZ-ring demonstrated by fluorescence recovery after photobleaching, *Proc. Natl. Acad. Sci. U.S.A. 99*, 3171−3175.
10. Errington, J., Daniel, R. A., and Scheffers, D. J. (2003) Cytokinesis in bacteria, *Microbiol. Mol. Biol. Rev. 67*, 52−65.
11. Corton, J. C., Ward, J. E., Jr., and Lutkenhaus, J. (1987) Analysis of cell division gene ftsZ (sulB) from Gram-negative and Gram-positive bacteria, *J. Bacteriol. 169*, 1−7.
12. Desai, A., and Mitchison, T. J. (1998) Tubulin and FtsZ structures: functional and therapeutic implications, *BioEssays 20*, 523−527.
13. Projan, S. J. (2002) New (and not so new) antibacterial targets—from where and when will the novel drugs come?, *Curr. Opin. Pharmacol. 2*, 513−522.
14. Beuria, T. K., Santra, M. K., and Panda, D. (2005) Sanguinarine blocks cytokinesis in bacteria by inhibiting FtsZ assembly and bundling, *Biochemistry 44*, 16584−16593.
15. Margalit, D. N., Romberg, L., Mets, R. B., Hebert, A. M., Mitchison, T. J., Kirschner, M. W., and RayChaudhuri, D. (2004) Targeting cell division: small-molecule inhibitors of FtsZ GTPase perturb cytokinetic ring assembly and induce bacterial lethality, *Proc. Natl. Acad. Sci. U.S.A. 101*, 11821−11826.
16. Wang, J., Galgoci, A., Kodali, S., Herath, K. B., Jayasuriya, H., Dorso, K., Vicente, F., Gonzalez, A., Cully, D., Bramhill, D., and Singh, S. (2003) Discovery of a small molecule that inhibits cell division by blocking FtsZ, a novel therapeutic target of antibiotics, *J. Biol. Chem. 278*, 44424−44428.

17. White, E. L., Suling, W. J., Ross, L. J., Seitz, L. E., and Reynolds, R. C. (2002) 2-Alkoxycarbonyl aminopyridines: inhibitors of *Mycobacterium tuberculosis* FtsZ, *J. Antimicrob. Chemother. 50*, 111−114.
18. Bendall, J. G., and Cambie, R. C. (1995) Totarol: a non-conventional diterpenoid, *Aust. J. Chem. 48*, 883−917.
19. Kubo, I., Muroi, H., and Himejima, M. (1992) Antibacterial activity of totarol and its potentiation, *J. Nat. Prod. 55*, 1436−1440.
20. Constantine, G. H., Karchesy, J. J., Franzblau, S. G., and LaFleur, L. E. (2001) (+)-Totarol from *Chamaecyparis nootkatensis* and activity against *Mycobacterium tuberculosis*, *Fitoterapia 72*, 572−574.
21. Kubo, I., Muroi, H., and Kubo, A. (1994) Naturally occurring anti-acne agents, *J. Nat. Prod. 57*, 9−17.
22. Haraguchi, H., Oike, S., Muroi, H., and Kubo, I. (1996) Mode of antibacterial action of totarol, a diterpene from *Podocarpus nagi*, *Planta Med. 62*, 122−125.
23. Shapiro, S., and Guggenheim, B. (1998) Inhibition of oral bacteria by phenolic compounds. Part 1. QSAR analysis using molecular connectivity, *Quant. Struct.-Act. Relat. 17*, 327−337.
24. Micol, V., Mateo, C. R., Shapiro, S., Aranda, F. J., and Villalain, J. (2001) Effects of (+)-totarol, a diterpenoid antibacterial agent, on phospholipids model membranes, *Biochim. Biophys. Acta 1511*, 281−290.
25. Evans, G. B., Furneaux, R. H., Gainsford, G. J., and Murphy, M. P. (2000) The synthesis and anti bacterial activity of totarol derivatives. Part 3: Modification of ring-B, *Bioorg. Med. Chem. 8*, 1663−1675.
26. White, E. L., Ross, L. J., Reynolds, R. C., Seitz, L. E., Moore, G. D., and Borhani, D. W. (2000) Slow polymerization of *Mycobacterium tuberculosis* FtsZ, *J. Bacteriol. 182*, 4028−4034.
27. Santra, M. K., Beuria, T. K., Banerjee, A., and Panda, D. (2004) Ruthenium red-induced bundling of bacterial cell division protein, FtsZ, *J. Biol. Chem. 279*, 25959−25965.
28. Beuria, T. K., Krishnakumar, S. S., Sahar, S., Singh, N., Gupta, K., Meshram, M., and Panda, D. (2003) Glutamate-induced assembly of bacterial cell division protein FtsZ, *J. Biol. Chem. 278*, 3735−3741.
29. Bradford, M. M. (1976) A rapid and sensitive method for the quantitation of microgram quantities of protein utilizing the principle of protein-dye binding, *Anal. Biochem. 72*, 248−254.
30. Geladopoulos, T. P., Sotiroudis, T. G., and Evangelopoulos, A. E. (1991) A malachite green colorimetric assay for protein phosphatase activity, *Anal. Biochem. 192*, 112−116.
31. Mukherjee, A., Santra, M. K., Beuria, T. K., and Panda, D. (2005) A natural osmolyte trimethylamine N-oxide promotes assembly and bundling of the bacterial cell division protein, FtsZ and counteracts the denaturing effects of urea, *FEBS J. 272*, 2760−2772.
32. Lee, J. C., Harrison, D., and Timasheff, S. N. (1975) Interaction of vinblastine with calf brain microtubule protein, *J. Biol. Chem. 250*, 9276−9282.
33. Gupta, K., Bishop, J., Peck, A., Brown, J., Wilson, L., and Panda, D. (2004) Antimitotic antifungal compound benomyl inhibits brain microtubule polymerization and dynamics and cancer cell proliferation at mitosis, by binding to a novel site in tubulin, *Biochemistry 43*, 6645−6655.
34. Gupta, K., and Panda, D. (2002) Perturbation of microtubule polymerization by quercetin through tubulin binding: a novel mechanism of its antiproliferative activity, *Biochemistry 41*, 13029−13038.
35. Mohan, R., Banerjee, M., Ray, A., Manna, T., Wilson, L., Owa, T., Bhattacharyya, B., and Panda, D. (2006) Antimitotic sulfonamides inhibit microtubule assembly dynamics and cancer cell proliferation, *Biochemistry 45*, 5440−5449.
36. Skehan, P., Storeng, R., Scudiero, D., Monks, A., McMahon, J., Vistica, D., Warren, J. T., Bokesh, H., Kenney, S., and Boyd, M. R. (1990) New colorimetric cytotoxicity assay for anticancer drug screening, *J. Natl. Cancer Inst. 82*, 1107−1112.
37. Mukherjee, A., and Lutkenhaus, J. (1994) Guanine nucleotide-dependent assembly of FtsZ into filaments, *J. Bacteriol. 176*, 2754−2758.
38. Mingorance, J., Rueda, S., Gomez-Puertasm, P., Valencia, A., and Vicente, M. (2001) *Escherichia coli* FtsZ polymers contain mostly GTP and have a high nucleotide turnover, *Mol. Microbiol. 41*, 83−91.
39. Yu, X. C., and Margolin, W. (1998) Inhibition of assembly of bacterial cell division protein FtsZ by the hydrophobic dye 5,5′-bis-(8-anilino-1-naphthalenesulfonate), *J. Biol. Chem. 273*, 10216−10222.
40. Gunderson, S. M., Hayes, R. A., Quinn, J. P., and Danziger, L. H. (2004) In vitro pharmacodynamic activities of ABT-492, a novel quinolone, compared to those of levofloxacin against *Streptococcus pneumoniae*, *Haemophilus influenzae*, and *Moraxella catarrhalis*, *Antimicrob. Agents Chemother. 48*, 203−208.
41. Turner, J., Cho, Y., Dinh, N. N., Waring, A. J., and Lehrer, R. I. (1998) Activities of LL-37 a cathelin-associated antimicrobial peptide of human neutrophils. *Antimicrob. Agents Chemother. 42*, 2206−2214.
42. Urgaonkar, S., La Pierre, H. S., Meir, I., Lund, H., RayChaudhuri, D., and Shaw, J. T. (2005) Synthesis of antimicrobial natural products targeting FtsZ: (±)-dichamanetin and (±)-2‴-hydroxy-5″-benzylisouvarinol-B, *Org. Lett. 7*, 5609−5612.
43. Ito, H., Ura, A., Oyamada, Y., Tanitame, A., Yoshida, H., Yamada, S., and Wachi, assembly of bacterial cell division protein FtsZ in vitro and in vivo, *Microbiol. Immunol.* 50, 759−764.

BI602573E